Team Results Document

SenseNC

NC STATE UNIVERSITY

Team Members:
McKenna Downey
Grace Maddocks
Sucheta Malladi
Kaila Peterson
Shannon Pinnell
Meredith Robbins
Sydney Stine
Joshua Wilson

Supervisors:
Dr. Michael Daniele
Dr. Stefano Menegatti

Coaches:
Katie Kilgour
Brendan Turner

August 17, 2021

SensUs

Abstract

H1N1, commonly known as Swine Flu, is an influenza type A virus characterized by rapid airborne transmission and high rates of infection. This high infection rate increases the need for efficient testing methods. Current solutions for detection are limited in their ability to provide at-home rapid testing. Our work aims to create a novel biosensor system that detects the presence of H1N1 in a saliva sample with a hemagglutinin aptasensor. Within the capsid of a given H1N1 particle, hemagglutinin (HA) is the most abundant protein antigen; therefore, the use of HA is a prime target for detection of H1N1 viral load. The presented biosensor utilizes a redox modified aptamer and custom electrochemical instrumentation. The RHA0006 DNA aptamer was used as a template for modifications upon which both thiol and methylene blue attachments were added. This aptamer was previously reported to exhibit high sensitivity and specificity to HA. The custom electrochemical instrumentation was designed and engineered to provide benchtop, portable interrogation of the aptasensor. Quantification of HA, within the estimated range for 10^{-10} virus particles/mL was evaluated by square wave voltammetry. Operation of the aptasensor was conducted with a commercial potentiometer and the custom electrochemical instrumentation and results were compared.

1. Biosensor System and Assay

Overview. The fundamental principle behind our sensor is that an electrode functionalized with a redox-modified aptamer will indicate a change in electrical response based on binding to the target analyte when placed in solution. Specifically, we developed a label-free square-wave voltammetry (SWV) aptasensor to detect HA, in which an anti-HA-aptamer was used as a molecular recognition element, and methylene blue (MB) as a redox probe. At the bare gold electrode, the redox probe can be easily accessed at the electrode surface to generate a SWV signal. At the anti-HA-aptamer electrode surface, when HA is present, the binding of the analyte results in a change in the availability for a redox reaction depending on the aptamer-antigen conformation, which results in a changed SWV current, see **Figure 1.** Section 2 provides a detailed explanation of the principles behind each stage of the sensor concept proposed herein: molecular recognition, physical transduction via electrodes, cartridge technology, and final readout.

Molecular Recognition and Assay Reagents. Hemagglutinin (HA) was the protein target to be sensed in samples of human saliva because it is the most abundant antigen on the surface of any given H1N1 particle [1]. The molecular recognition of HA is accomplished by RHA0006 aptamer, sequence 5'-GGGTTTGGGTTGGGTTGGGTTTTTGGGTTTGG GTTGGGTTGGGAAAAA-3'; the prediction of secondary structure is shown in **Figure 2 ()**. This aptamer was selected because of the reported high binding affinity of $1.53x10^{-8}$ M to hemagglutinin [2]. Another advantage of this aptamer lies in the fact that it is a DNA aptamer, which provides increased stability over an RNA aptamer option [2]. In **Figure 2**, the RHA0006 aptamer is seen bound to the extracellular domain of the rHA, which is a composition of two different strains of the HA protein. Methylene blue and thiol modifications were made to the selected RHA0006 aptamer. The thiol group was essential in allowing the aptamer to bind to the gold surface of the electrodes on the biosensor. Methylene blue was also an important modification to the aptamer because it serves as a redox probe to interrogate any conformational changes from the formation of the aptamer-HA complex. Methylene blue exhibits a peak reduction potential at -0.25V [3]. Surface Plasmon Resonance (SPR) was used to calculate the binding constant for the chosen aptamer to HA in our laboratory testing environment with a BioNavis SPR machine. Detailed procedure and results can be found in Section 2, "Technological Feasibility."

Electrochemical Transduction. For both benchtop and final device testing, Metrohm Screen-Printed Electrodes, DRP-220BT, were used, see **Figure 3**. Before functionalization and testing, the electrodes were cleaned by running cyclic voltammetry from 0 to +1.2 V for 15 cycles on the electrode while the electrode surface was covered by a 0.5 M H_2SO_4 solution. For testing after the electrodes were functionalized, a solution was pipetted onto the full electrode surface, covering all three electrodes, to complete the cell. Then square wave voltammetry (SWV) was applied to the electrode from -0.4 V to +0.1 V, with a step size of 0.00015 V, a mod amp of 0.025 V, and a frequency of 50 Hz. The SWV measures the current response of the electrode to the applied voltage sweep under the set parameters. The measured current response will change due to modifications to the surface chemistry of the electrode; one simple example of a surface change is the functionalization with a biorecognition element (BE), in our case, the aptamer. More significantly, the sensor's

current response to a square wave voltage will change after a target-laden solution has been introduced to the functionalized electrode. The target induces a deformation in the aptamer which changes the position of methylene blue changing the working electrode's surface morphology and thus the magnitude of the SWV result.

Fluidic Cartridge. To increase design simplicity, fluid and sample handling complexity was kept to a minimum. The samples can come directly from the user without any pre-processing. Exposure of the device to the sample is conducted by simply placing a drop of saliva on the exposed electrode surfaces. Essentially, the saliva is used to complete the electrochemical cell. The electrodes described in the above section were explicitly chosen because of their ability to take measurements on samples on the order of 50 µL. When stimulated by chewing, human saliva is typically produced at a rate of ~5 mL per minute. Unstimulated rates lie on the order of 0.5 mL per minute [4]. Although salivation rates vary between subjects, the typical human is expected to hold ~0.87 mL (male) or ~0.66 mL (female) of saliva in their mouth at any given moment, on average [5]. As a result, the production of 50 µL, or 0.05 mL of saliva for a testing sample is a highly feasible requirement. Users can simply produce this spit sample into a provided cup and with a provided plastic pipet, place their spit onto the device. Users can be instructed to ensure that their spit covers all electrode areas, bridging all blue dielectric areas together, completing the cell and enabling electrical measurements. Electrodes will be shipped to the user already prepared with the aptamer monolayer, ready for use. Inspiration for this feature was drawn from glucose test strips, which come to the user already prepared with enzymes, ready to accept a sample [6].

Mobile Electrochemistry Instrument. To complete a measurement the user will turn on the device using a switch, and then be prompted to retrieve a testing strip. The user will place the test strip into the slot until it is firmly seated in. Once this is completed the user will be prompted to press a button so testing can begin. The slot will only physically allow the user to push the test strip into the desired depth- the channel is not long enough to facilitate pushing the test strip in too far.

Once the button is pressed this will prompt the internal electronics of the sensor to begin a testing sequence. First, the non-contact temperature sensor will take the temperature of the testing strip for use in post processing. At this point, the electrode leads on the testing strip will be in contact with the electrode and the AD5941 will be prompted by the onboard microcontroller to run the testing routines needed to perform Square Wave Voltammetry and Impedance Spectroscopy. The AD5941 will then relay these values to the onboard microcontroller where the measured values will be post-processed. This processing will include steps for using a previously created calibration table to calibrate the measurement and also include running correction equations for temperature bias - using measurements gathered from the temperature sensor.

If the device is set to display only the test result (likely in consumer settings), then a screen will appear showing the test results in-text, see **Figure 4** for all possible test results. Even though the user interface is easy to use and understand for many individuals, additional accessibility settings can be configured in the sensor menu. This can make the text larger or change the color scheme to accommodate those who are colorblind.

2. Technological Feasibility

Molecular Recognition. The molecular recognition aspect of our sensor began with testing how effectively our aptamer was able to bind to our intended target, HA. To further investigate the aptamer's binding capacity, we had to perform experiments to calculate its binding affinity, K_D, in the presence of HA. In finding this value, it further proved the usability of our selected aptamer for our sensor design. Once the K_D proved that the aptamer was effective, we were able to introduce it to the surface of our sensor electrodes in order to functionalize them for proper use and measurements of the HA protein.

Surface Plasmon Resonance (SPR). After the selection of the RHA0006 aptamer mentioned above, we were able to model its binding affinity using Surface Plasmon Resonance (SPR). Specific details of SPR procedures can be found under **Figure 5** in the Appendix. The K_D value for the RHA0006 aptamer was found to be 1.788×10^{-8} M when SPR was conducted in our laboratory setting. Future work will be conducted to increase the sample size of SPR data values. The BioNavis machine available to our team is not equipped with internal degassing measures, meaning that procedures had increased complexity in order to avoid bubbling within sample administration tubing. Additionally, calibration of the SPR machine was a recurrent issue; representatives from BioNavis recently provided information for proper recalibration, allowing our team to continue gathering more accurate and more plentiful SPR data.

Electrode Functionalization. The metrohm electrodes used for our sensor were functionalized following the same procedure as the SPR chip functionalization but with a smaller amount of fluid due to the metrohm electrode surface being smaller. **Figure 6** shows size comparisons between the SPR chips and metrohm electrodes and **Figure 7** is a visual representation of the functionalization process. Challenges involving the electrode functionalization and procedure were centered around the electrode-aptamer lifetime. It is a possibility that over time, after functionalization, the aptamer monolayer may not be indefinitely viable, as degradation may occur. Once the monolayer starts to degrade, the electrode slowly loses the ability to bind the HA protein as well, skewing the reading of the sensor. Further testing on our functionalized electrodes would need to be conducted to determine the exact viability over a desired time period. In the future, we hope to develop various characterization methods to ensure that the viability of the functionalized aptamer monolayer extends over longer periods of time.

Physical Transduction. With the electrode setup and test parameters detailed in Section 1, “BioSensor System and Assay”, established, data was collected from our sensor across a wide range of concentrations. Based on the binding constant presented by Shiratori, et.al. and the data collected by our laboratory’s own SPR experiments, testing was conducted from 10 nM to 1425 nM. Such high concentrations were included in order to explore the location at which our sensor may saturate, which is important in understanding feasibility of deployment into the commercial market. Discussion of Raw Square Wave Data and Results can be found under **Figure 8** in the Appendix. Two approaches were considered in deciding which data points should be extracted to determine concentration from current magnitude, both represented in **Figure 9**. Approach A involves calculating the maximum

current value across the entire square wave voltage window (-0.4 to +0.1 V) and relating this value to concentration. Approach B is more specific, relying on the presence of the methylene blue peak at -0.25 V, pulling the current magnitude at -0.25 Volts from the raw SWV data to correlate it to concentration. Feasibility implications of each, along with correlation plots and their R^2 values, are discussed after **Figure 9**, in the Appendix. The feasibility of our sensor concept is established by data showing successful transduction, presented in **Figure 8** and **Figure 9**. When our corresponding sensor hardware runs the established SWV protocol and pinpoints the maximum current across the applied voltage range, the value can be compared to a lookup table populated by data points on this trendline developed by our benchtop testing.

Moving forward, we plan to address some potential improvements to our signal transduction strategies. These include biologically accurate virus simulations, investigation into all elements of the selection buffer and their impact on the analyte, increase in data sample size, and introduction of additional electrochemical tests (EIS) to verify concentrations calculated from SWV results. Details of these areas for improvement and our team's strategies to address them are included in the Appendix, below **Figure 9**.

Fluidic Cartridge. Due to the simplicity of the fluidics involved in our proposed sensor, minimal data was collected on cartridge viability. Verification of electrode functionality when 55 µL or greater was verified throughout the square wave testing process. Additionally, several subjects were asked to attempt to place a fluid sample onto the electrode to test usability. Most users found the task easier with higher levels of fluid (around 100 µL, seen at right in **Figure 10**), which fits into reasonable salivation rates; additionally, this adjustment would allow for an increased likelihood of the user completely covering/completing the electrochemical cell during sample placement. Potential areas of improvement are discussed beneath **Figure 10**, in the Appendix.

Mobile Electrochemistry Instrument. Because the instrument reader is comprised of off the shelf components, the design is feasible. Additionally, because the components interface through established communication methods such as SPI and I2C there are established libraries to communicate between components and transfer data. We were able to connect an MSP430 microcontroller to an LCD screen and button to allow for data streams between the devices, see **Figure 11**. These are the main components of the system and successfully interfacing between them supports the feasibility of our design.

In feedback from potential users, a number of potential failure points were identified. First, the user may not fully understand the on screen text and animations and may not place the saliva onto the test strip in the appropriate way, may incorrectly place the strip into the device, or otherwise prevent an accurate measurement. In those we spoke with, the feasibility of the design proposed was not questioned, however there were concerns brought up around user interaction. Additionally, the temperature of the saliva sample is important to the results of the biosensor. Temperature measurements need to be performed on the sample while test events occur, and need to be extremely accurate. There is a flaw in user interaction and physical design that does not allow us to receive accurate temperature measurements. Finding solutions to these issues is extremely important for our future designs, our strategies of improvement are detailed with **Figure 11** in the appendix.

3. Originality

From the Team. The SenseNC biosensor approached the detection of H1N1, in a saliva sample, with a combination of electrical and chemical novelty. Our team was able to identify an aptamer able to specifically bind to Hemagglutinin, and after careful literature review we purchased this aptamer to begin testing. Once we gained the ability to bind specifically to our target then we needed a way to physically manipulate the location of Hemagglutinin within the saliva sample. The SenseNC team decided to use impedance spectroscopy and square wave voltammetry to physically manipulate the location of the Hemagglutinin to determine the concentration of H1N1. The AD5941 and MSP430 were purchased as the electrical hardware to perform the physical analysis. The team was able to incorporate the two electronic hardware components together, with the specified aptamer, to develop a unique biosensor.

From the Supervisor

The hemagluttanin (HA) aptasensor utilizes a square wave voltammetry electrochemical method, which has not been demonstrated previously for the HA-aptamer complex. Typical HA aptasensors use colorimetric transduction (i.e. lateral flow assay) or impedance spectroscopy. All biochemical assays, electrochemical testing, hardware design, fabrication, and testing were carried out by the Team. The Faculty Supervisors and Team Guides provided guidance and access to laboratory instrumentation and protocols, along with funds for material procurement. The team worked with their Faculty Supervisors to conceive the aptasensor, and the Team independently carried out the research and development objectives. Testing of the electrochemical sensors, complete development of the electronic hardware, investigation of the translation potential, and completion of all SensUs requirements were completed nearly 100% independently by the members of the Team.

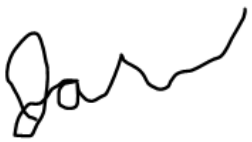

4. Translation Potential

Business Model Canvas

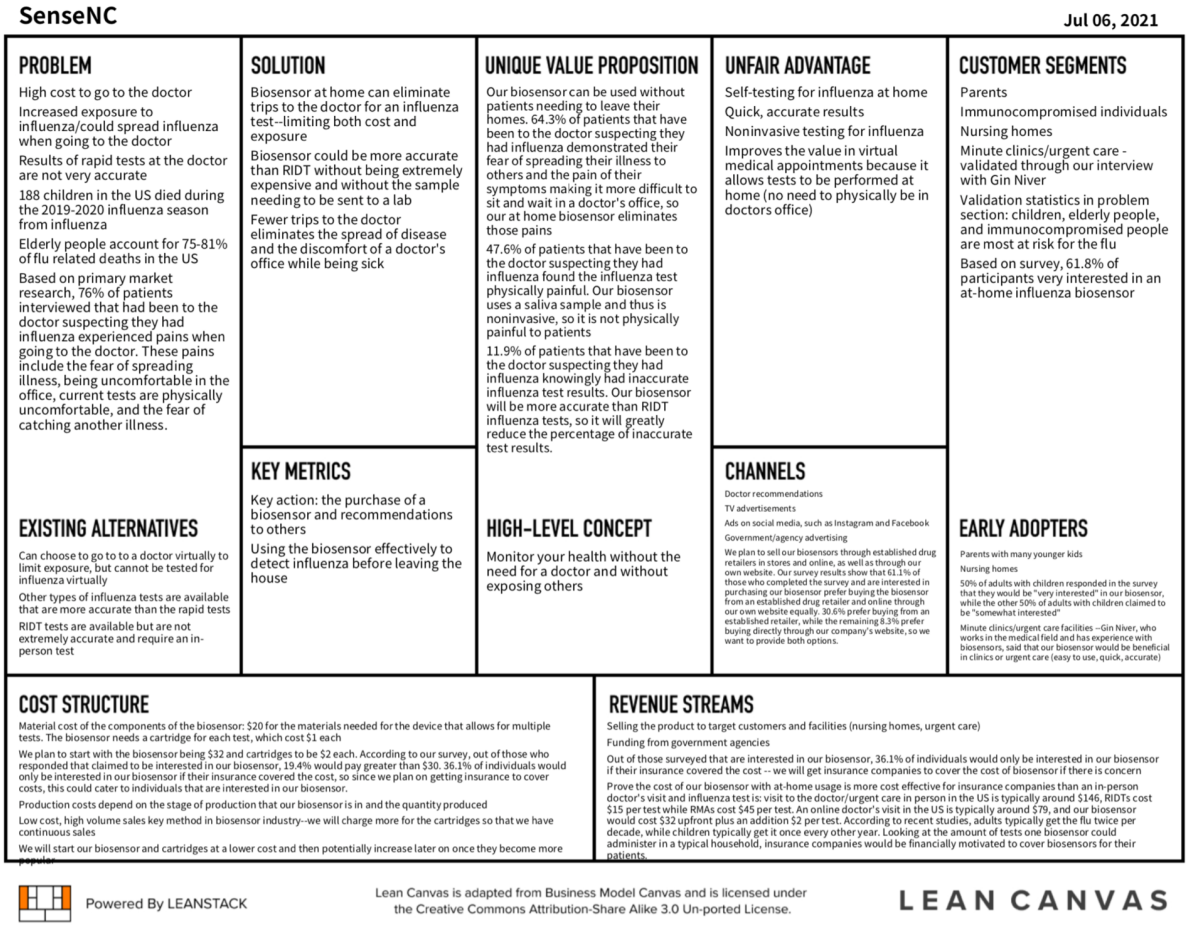

Market Description. In the United States of America, the Food and Drug Administration (FDA) regulates the performance and marketing of a medical device. Our biosensor must follow strict manufacturing and engineering guidelines to ensure that customers are not harmed. the claimed performance is met, and all personal medical records are secure. Following the FDA's protocol, the biosensor is considered a medical device as it is intended to diagnose a disease and prevent the transmission of the virus. FDA's Center for Devices and Radiological Health (CDRH) is responsible for regulating the development, manufacture, repackage, relabel, and/or import of medical devices sold in the United States.

Based on our conversation with Gin Niver (an American medical professional) the healthcare system is actively seeking to bring healthcare to homes. Medical devices are in extreme demand, and our biosensor will be able to diagnose customers without needing to enter a doctors office. We will allow customers to purchase our product online and hope to include physicians in diagnosis.

Stakeholder Desirability. Patients are currently tested for influenza upon noticing symptoms and going to the doctor, where they receive either a Rapid Influenza Diagnostic Test (RIDT) or a Rapid Molecular Assay (RMA). Customer pains for going to the doctor to get an influenza test currently include the fear of spreading their illness or catching another illness, being uncomfortable in the office, current tests are physically uncomfortable and invasive, and current tests are not always accurate. Our biosensor that can detect H1N1 from a saliva sample eliminates these pains associated with traveling to a doctor's office to receive a RIDT or RMA since our biosensor can be used at home and is more accurate than RIDTs or RMAs. Additionally, RIDTs and RMAs are both invasive tests, while our biosensor is a non-invasive test, eliminating discomfort associated with current influenza tests.

In terms of cost, our biosensor is more effective than RIDTs and RMAs as well. A visit to the doctor or urgent care in person in the US is typically around $146 [9]. RIDTs cost $15 per test while RMAs cost $45 per test [10]. An online doctor's visit in the US is typically around $79 [9], and our biosensor would cost $32 upfront plus an additional $2 per test. Thus going to the doctor to get a RIDT typically costs around $161 and going to the doctor to get a RMA typically costs around $191, while attending a virtual doctor's visit and purchasing our biosensor would be $113, and only $81 for each test and virtual visit combined after the initial purchase.

Patients will value our biosensor over other testing methods because it is more accurate and eliminates pains of discomfort and traveling to the doctor's office. Doctors will benefit from our biosensor as well because it saves time and reduces the number of patients they need to interact with in person for an appointment that can be done virtually. Our at-home biosensor eliminates the transmission of the flu between different patients and between patients and doctors, which can be specifically helpful since the H1N1 virus is so contagious. Our biosensor is also beneficial for insurance companies because of the cost savings that they would experience from funding a biosensor and a virtual appointment instead of funding a visit to the doctor and either a RIDT or RMA.

Business Feasibility. Our main resources used have been NC State labs and materials. We also spoke to a medical professional to get advice about the market for biosensors, who helped bring up the idea that biosensors could be very useful in urgent care or clinics because they are quick, accurate, and easy to use. These resources have allowed us to both create our biosensor and make a business model for it. We would intend to further utilize the NC State entrepreneurship facilities to prototype and develop our biosensor technology. Specifically, he NC State Entrepreneurship Garage is a venture creation and prototyping space designed for student entrepreneurs. It serves as a hub for students across campus to come together and explore their entrepreneurial ideas and interests. In partnership with Raleigh Founded, students call the Garage home to work on challenges alongside non-university businesses.

This startup space has a physical space for entrepreneurs to develop, create and invent as well as programmatic resources like community meet-ups and skills workshops, which would be necessary to build out partners in manufacturing, regulation, marketing, and clinical testing.

In order to produce our biosensor on a larger scale, we also need to consult with experts on FDA regulations, marketing, and manufacturing. Manufacturing of similar electrochemical

sensors and test-strips have been provided by contract medical research and manufacturing organizations (CMRMOs), such as Zimmer and Peacock. The basic chemistry and materials of our sensor are commercially available, and all fabrication processes are industrially scalable. Quality control of the sensor surface will be paramount in the production pipeline, as each batch of sensors will need to be calibrated and the Mobile Electrochemistry Instrument will need to be updated with this calibration information. Similar to glucose meters, the calibration information can be downloaded to the Mobile Electrochemistry Instrument via wireless connectivity or a supplemental memory stick.

When marketing our biosensor, we intend to target it towards insurance companies, healthcare professionals, and urgent care clinics, as well as nursing homes and parents with younger children. This way healthcare professionals can suggest our biosensor to patients, insurance can cover the costs, and nursing homes can use it within the facility and parents especially can use our biosensor in their homes. We will make sure to keep our relationships with insurance providers and medical professions to receive feedback on our biosensors and be a best in class provider for patients.

Financial Viability. Our biosensor will be sold through established drug retailers in stores and online, as well as through our own website. Our team conducted a survey, and the results show that 61.1% of those who completed the survey and are interested in purchasing our biosensor prefer buying the biosensor from an established drug retailer and online through our own website equally. 30.6% prefer buying from an established retailer, while the remaining 8.3% prefer buying directly through our company's website, so we want to provide both options.

We estimate that the cost of the biosensor will be $20 for materials and an additional $1 cost for each cartridge. We plan to charge $32 for our biosensor and $2 for each cartridge. We plan to use a low cost, high volume sales key method that is often used in the biosensor industry: we will charge more for the cartridges eventually so that we can maintain continuous sales. We are also starting both our biosensor and cartridges at a lower cost and may raise them later on depending on sales. According to our survey, out of those who responded that claimed to be interested in our biosensor, 19.4% would pay greater than $30. 36.1% of individuals would only be interested in our biosensor if their insurance covered the cost, so since we plan on getting insurance to cover costs, this could cater to individuals that are interested in our biosensor. We are planning to have insurance cover the cost of our biosensor for patients with the financial proof (provided in *Stakeholder Desirability*) that on average a patient purchasing our biosensor for an influenza test is less expensive than them going to the doctor for a RIDT or RMA and would save them even more money long term.

5. Team and support

Dr. Michael Daniele and Dr. Stefano Menegatti:
Michael Daniele and Stefano Menegatti are the team's supervisors. They provide guidance on technical decisions, instruction and resources for team members to seek advice.
Katie Kilgour and Brendan Turner:
Katie Kilgour and Brendan Turner are team coaches and assist team members throughout the completion of the biosensor by providing technical support.
Meredith Robbins:
Meredith Robbins is the business team lead and is responsible for promoting our team's success on social media and providing financial support. She has been an integral part of developing our business model, to ensure that our product will be successful.
Sydney Stine:
Sydney Stine is a chemistry team member. Sydney researches and designs an aptamer that binds to Hemagglutinin in order to create an electrochemical sensor. Responsibilities include aptamer selection and in-lab testing relating to the aptamer and its binding efficiency.
McKenna Downey:
McKenna Downey is a chemistry team member. McKenna contributes to the design and testing of sensor hardware and the interface between the surface chemistries, binding, and how this can be transduced to be understood by electronics. Responsibilities include solution preparation, electrode fabrication and benchtop testing, including SWV and SPR.
Kaila Peterson:
Kaila Peterson is an electrical team member. Kaila designs and tests sensor hardware and corresponding software. Responsibilities include electrode selection and fabrication, in-lab testing, and sensor/controller interfacing.
Grace Maddocks:
Grace Maddocks is an electrical team member who works closely with the chemical team. Grace contributes to the design and testing of sensor hardware and the interface between the surface chemistries, binding, and how this can be transduced to be understood by electronics. Responsibilities include electrode fabrication and benchtop testing, including SWV and SPR.
Shannon Pinnell:
Shannon Pinnell is an electrical team member. Shannon contributes hardware design that allows the team to take square wave voltammetry and impedance spectroscopy measurements. Some data analysis and PCB design.
Sucheta Malladi:
Sucheta Malladi is an electrical team member. Sucheta designs hardware and software that will perform square wave voltammetry and impedance spectroscopy. PCB design / embedded software / power system, testing, and implementation.
Joshua Wilson:
Josh is the team captain and communicates changes made by the SensUs organization, ensures team goals are achieved, and tracks team progress. Josh is also an electrical team member and designs hardware and software that will perform square wave voltammetry and impedance spectroscopy.

6. Final Remarks

While the reported aptastensor shows promising response to hemagglutinin, we intend to proceed with future studies to improve both the linear detection and dynamic range of our sensor. After the competition, we will specifically investigate the use of high-surface area gold electrodes to extend the dynamic range by presentation of more aptamer and increasing the magnitude of the realized current; moreover, we we intend to simulate the sensing of H1N1 particulate by covalently-coupling the hemagglutinin protein to the surface of polymer nanoparticles (*diameter* ~10 nm). This simulation will better represent the sensor response to the hemagglutinin integral to the H1N1 capsid. We hypothesize that the interaction of the aptamer with the hemagglutinin functionalized particles will induce a larger conformational change, resulting in a greater magnitude change in the SWV current which translates to improved sensitivity.

Most importantly, the SenseNC Team would like to thank Dr. Banghyun Lee and Dr. Joe Lavoie for invaluable guidance and instruction on the use and interpretation of SPR and sensor data.

7. References

[1] Russier, Marion, Guohua Yang, Atanaska Marinova-Petkova, Peter Vogel, Bryan S. Kaplan, Richard J. Webby, and Charles J. Russell. “H1N1 Influenza Viruses Varying Widely in Hemagglutinin Stability Transmit Efficiently from Swine to Swine and to Ferrets.” PLoS Pathogens 13, no. 3 (March 10, 2017): e1006276. https://doi.org/10.1371/journal.ppat.1006276.

[2] Shiratori, Ikuo, Joe Akitomi, David A. Boltz, Katsunori Horii, Makio Furuichi, and Iwao Waga. “Selection of DNA Aptamers That Bind to Influenza A Viruses with High Affinity and Broad Subtype Specificity.” Biochemical and Biophysical Research Communications 443, no. 1 (January 3, 2014): 37–41. https://doi.org/10.1016/j.bbrc.2013.11.041.

[3] “Methylene Blue as a Novel Electrochemical Hybridization Indicator - Erdem - 2001 - Electroanalysis - Wiley Online Library.” Accessed August 17, 2021. https://analyticalsciencejournals.onlinelibrary.wiley.com/doi/epdf/10.1002/1521-4109%28200103%2913%3A3%3C219%3A%3AAID-ELAN219%3E3.0.CO%3B2-7.

[4] Iorgulescu, Gabriela. “Saliva between Normal and Pathological. Important Factors in Determining Systemic and Oral Health.” Journal of Medicine and Life 2, no. 3 (2009): 303–7.

[5] “The Volume of Saliva in the Mouth Before and After Swallowing - F. Lagerlof, C. Dawes, 1984.” Accessed August 17, 2021. https://journals.sagepub.com/doi/10.1177/002203458406300502?url_ver=Z39.88-2003&rfr_id=ori%3Arid%3Acrossref.org&rfr_dat=cr_pub++0pubmed&.

[6] Alto, William A., Daniel Meyer, James Schneid, Paul Bryson, and Jon Kindig. “Assuring the Accuracy of Home Glucose Monitoring.” The Journal of the American Board of Family Practice 15, no. 1 (January 1, 2002): 1–6.

[7] Kim, Yoon-Jin, Yeon Seok Kim, Javed H. Niazi, and Man Bock Gu. “Electrochemical Aptasensor for Tetracycline Detection.” Bioprocess and Biosystems Engineering 33, no. 1 (August 23, 2009): 31. https://doi.org/10.1007/s00449-009-0371-4.

[8] Zamay, Galina S., Tatiana N. Zamay, Vasilii A. Kolovskii, Alexandr V. Shabanov, Yury E. Glazyrin, Dmitry V. Veprintsev, Alexey V. Krat, et al. “Electrochemical Aptasensor for Lung Cancer-Related Protein Detection in Crude Blood Plasma Samples.” Scientific Reports 6, no. 1 (October 2016): 34350. https://doi.org/10.1038/srep34350.

[9] GoodRx. “How Much Does a Telehealth Visit Cost?” Accessed August 17, 2021. https://www.goodrx.com/telehealth/how-much-does-telehealth-cost.

[10] Svoboda, Elizabeth. “A Sticking Point for Rapid Flu Tests?” Nature 573, no. 7774 (September 18, 2019): S56–57. https://doi.org/10.1038/d41586-019-02754-7.

8. Appendix

Contained in this appendix are all figures and tables referenced within this body of work along with their corresponding captions. In addition, **relevant presentations and discussions of data and procedures are included subsequent to related figures.**

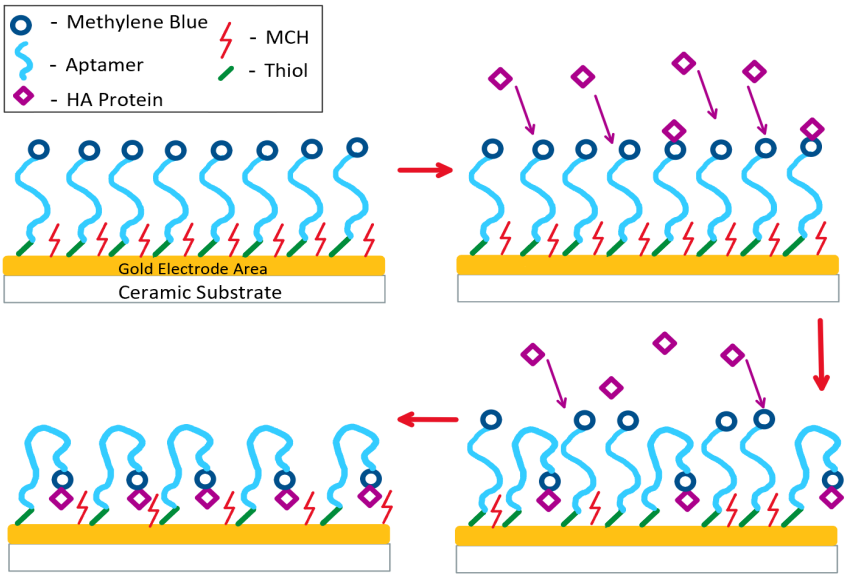

Figure 1. Top Left: Thiol and Methylene Blue modified aptamers functionalized to the surface of the gold electrode with methylcyclohexanol (MCH) used for blocking. Top Right: HA Protein is added onto the electrode. Bottom Right: HA Protein begins binding to the modified aptamer, causing it to change shape. Bottom Left: Electrode has reached saturation when all available aptamers have bound HA protein.

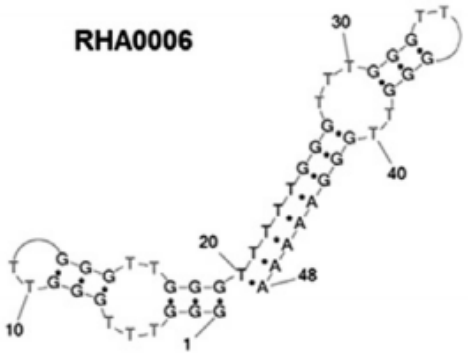

Figure 2. RHA0006 Aptamer Structure based on ValFold prediction of secondary structure as determined by Shiratori, et.al. [2]

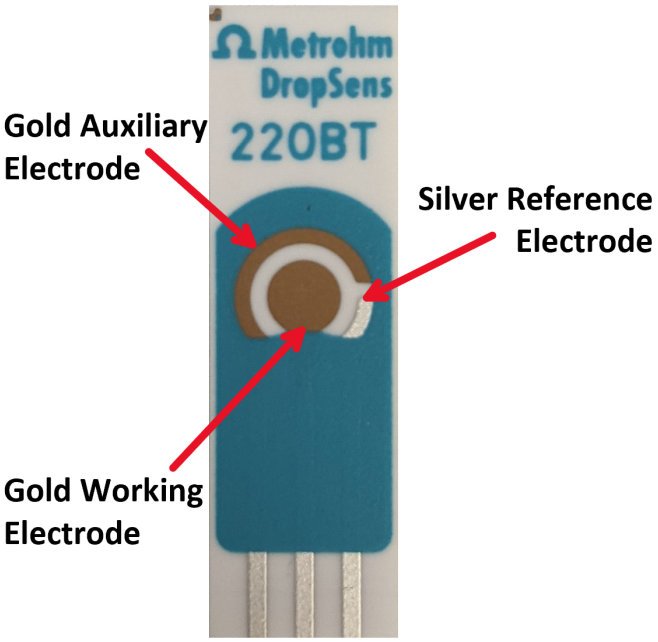

Figure 3. Metrohm Screen-Printed Gold Electrode (Au working, Au auxiliary, Ag/AgCl reference) were inserted into a DropSens screen-printed electrode connector interfaced with a Metrohm Autolab PGSTAT128N potentiostat to run all cleaning and testing procedures.

Figure 4. Device output to user for each possible test result.

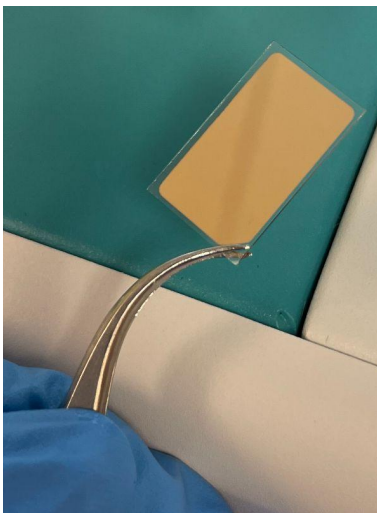

Figure 5. BioNavis SPR Gold Chip, 12 x 20 mm.

To perform SPR, our team used 12 x 20mm uncoated gold SPR chips, sourced from BioNavis and seen in **Figure 5**, functionalized with our aptamer. This process consisted of reducing 3 µL of the RHA0006 aptamer with an equal part 20 mM tris(2-carboxyethyl)phosphine (TCEP) solution. 300 µL of aptamer solution is needed for each chip so after the aptamer has been reduced, it is suspended in 1 mM $MgCl_2$ in 1x PBS to reach the desired volume. The gold surfaces of the SPR chips were gently cleaned using washes of acetone, ethanol and Milli-Q water for 60 seconds each and then dried with N_2 gas. The aptamer solution was carefully pipetted onto the gold surface of the chip to establish steady surface tension of the solution and ensure it is only touching the gold side. The gold chips with aptamer solution were left in a damp environment at room temperature for overnight incubation in dark conditions. After overnight incubation, a blocking step was conducted to block any other surface molecules other than the aptamer. This was done by first gently washing the aptamer solution off of the surface of the chip with Milli-Q water and drying it with N_2 gas. A 300 µL solution of 2 mM methylcyclohexane (MCH) was made in 1x PBS. The MCH was pipetted onto the surface of the chip and left to incubate in dark conditions for 1 hour. After incubation, the MCH was rinsed off of the chip using Milli-Q water for 60 seconds and it was dried with N_2 gas. The chip was then ready to use for SPR.

In running SPR reactions, 8 different concentrations of our HA protein were used to create an effective binding curve. The HA solutions were prepared using a selection buffer consisting of 50 mM Tris–HCl, pH 7.4, 100 mM NaCl, 5 mM KCl, 1 mM MgCl2, 0.01% Tween 20 [2]. The binding curve from each concentration used in SPR with the gold chips was analyzed to find the response unit (RU), which was the difference between the starting and ending baselines. These RU values were plotted against their concentration values and a ligand binding one site saturation regression was used to determine the value of the binding constant of our aptamer in the presence of HA, K_D.

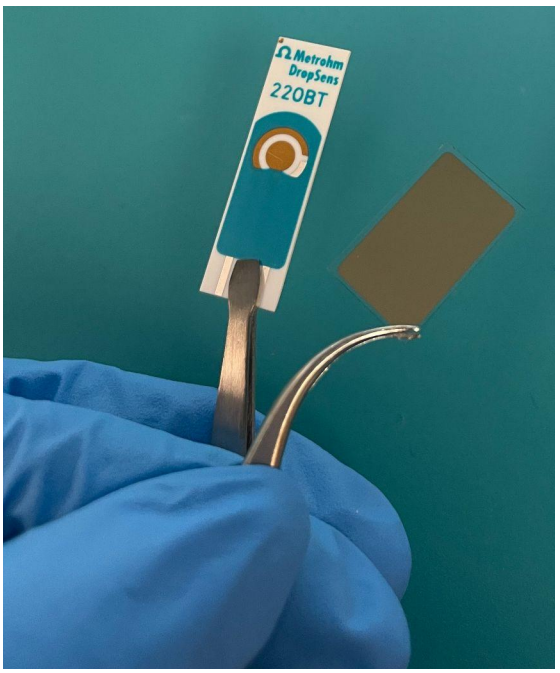

Figure 6. Metrohm electrode next to the BioNavis SPR chip for size comparison purposes.

The metrohm electrodes, mentioned previously, have a small circular gold electrode surface that was functionalized and introduced to the aptamer through the same process as the gold chips. The main difference between the two functionalization processes was the size of the functionalization surface, which can be seen in **Figure 6**. The small gold circle, the working electrode, seenin the middle of the blue electrode, is significantly smaller than the surface area of the entire gold rectangular SPR chip to its right. Since the electrode gold surface was smaller than the chips, a smaller volume of the aptamer solution was needed to cover the entire surface. Along with a smaller volume, more precision was necessary when pipetting to ensure the surface was not only fully covered but that the surface of the working electrode was not scratched or harmed. Incubation conditions were also kept the same, ensuring that incubation was kept in dark conditions. After the overnight incubation, the blocking step was also performed on the electrode surface using smaller volumes of MCH compared to the SPR chips. After blocking, the metrohm electrode was ready for square wave testing and introduction to the HA protein, see **Figure 7**.

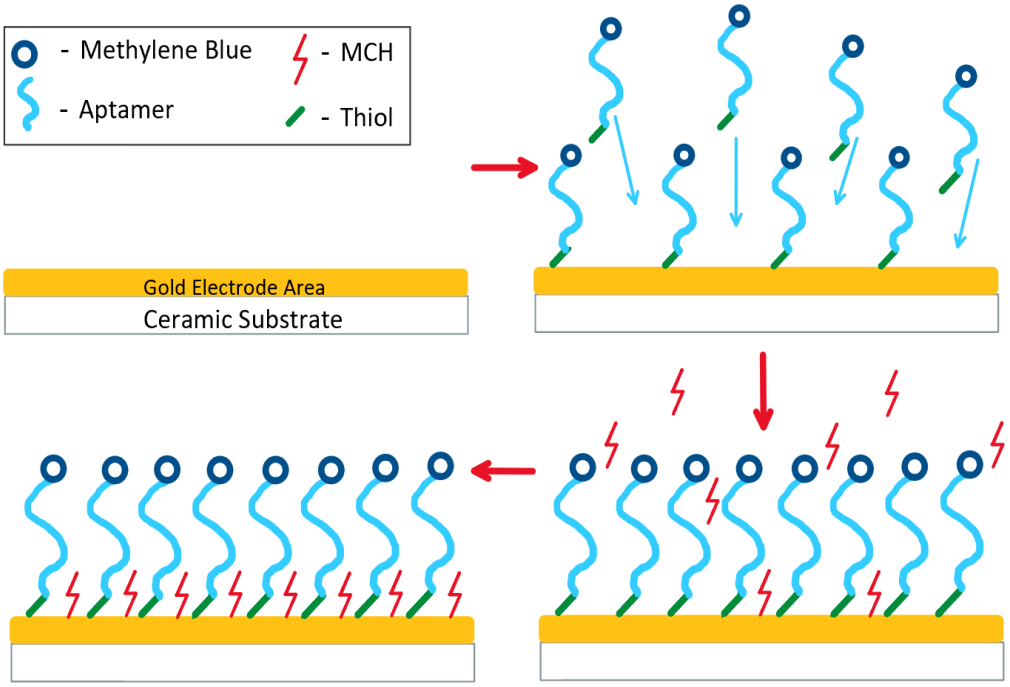

Figure 7. Top Left: Bare gold electrode on ceramic substrate. Top Right: Aptamer solution is added onto the gold surface where the thiol end binds to the gold. Bottom Right: After aptamer binding, an MCH solution is added to the electrode to block in the gaps. Bottom Left: Electrode after MCH blocking.

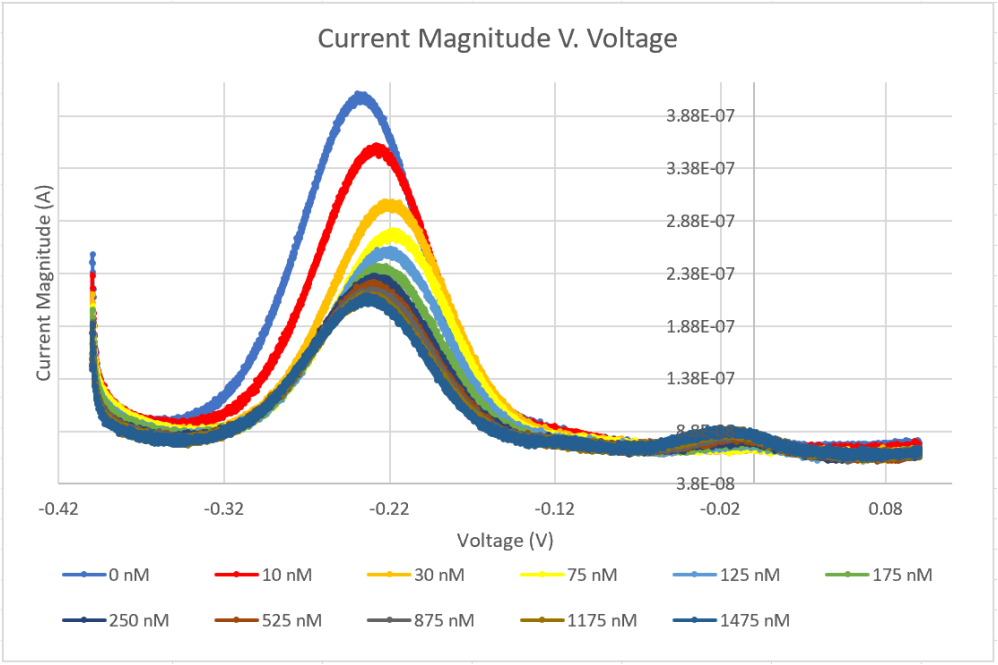

Figure 8A. Current V. Voltage of full concentration range. See discussion and analysis on the following page.

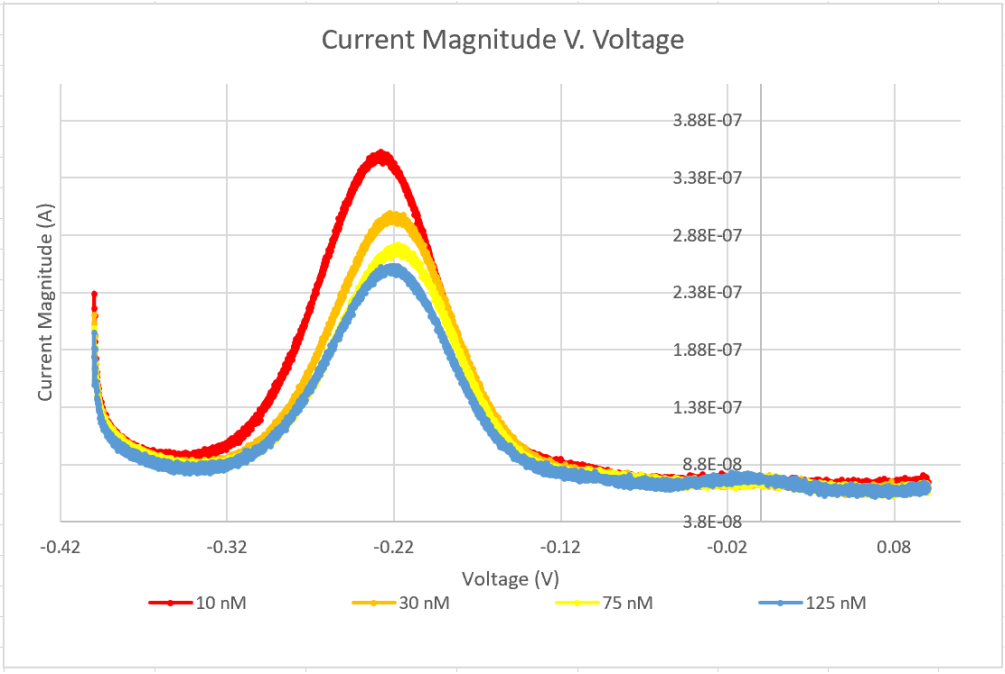

Figure 8B. Current V. Voltage of lower concentration ranger. See discussion and analysis on the following page.

Discussion of Figure 8 (SWV) Results.

Raw square wave results are plotted as current magnitude over voltage. Results across the entire concentration range can be seen in **Figure 8A**. **Figure 8B** shows the same results, adjusted to show only the lower concentrations, which are of interest for biological relevance. As seen in those figures, the magnitude of the square wave current peak consistently decreases as higher concentrations are introduced. This decrease in peak magnitude is expected as increasing quantities of HA bind to aptamers, causing them to deform towards the sensor surface, reducing the electron flow rate and thus the detectable current magnitude. Notably, similar results showing decreasing current magnitude with increasing analyte concentration have been obtained by other groups utilizing aptasensors with electrochemical SWV transduction. [7] [8]

The horizontal location of this peak is directly correlated with the presence of a Methylene Blue modification on the RHA0006 aptamer, as discussed previously. From this information, patterns can be pulled to correlate concentrations with certain data points to inform our sensor hardware.

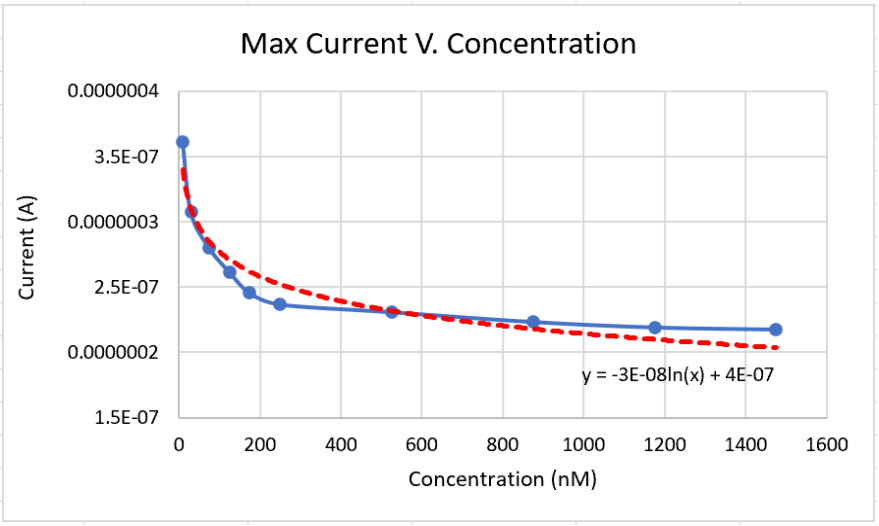

Figure 9A. Maximum current values at each concentration over the entire voltage sweep window.

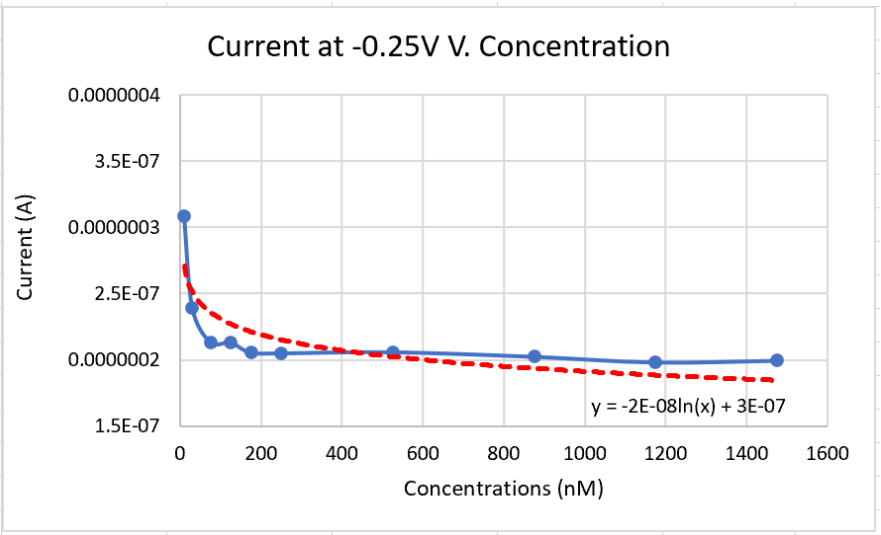

Figure 9B. Current value of each concentration at -0.25 V.

Discussion of Figure 9 Results.

Due to the saturation of the sensor as samples approach µM HA concentrations, a logarithmic trend line was most appropriate. In both Approach A and Approach B, a trend line was fitted and is indicated in **Figure 9**. Notably, Approach A showed an R^2 value of 0.9284, significantly higher than that of Approach B, R^2 = 0.6996.

Potential Areas of Improvement for Electrochemical Transduction Strategies.

Our sensor has been designed to specifically and sensitively bind and measure the HA protein molecule that is found on the surface of the H1N1 viral molecule. Thus the sensor is very applicable in the presence of the HA protein; however, it is unknown how the sensor will respond in the presence of the full, more complex, H1N1 virus. A solution for this problem, will be the attachment of HA molecules to nanoparticles, which will simulate a more biologically accurate viral particle and will test our sensor's viability to detect H1N1 as it presents in realistic human saliva samples. Another problem involving the physical transduction of the sensor is the different baselines that can occur for each individual electrode. In current experiments, the electrode baselines do not always start at the same value even though they are the same type of electrode and are functionalized identically. Our approach to resolving this problem would be to collect multiple sets of normalized data by having the user first expose the electrode to a 0 concentration and then proceed with their saliva. This would help generate a calibration for the sensor to gain the most accurate HA concentration reading. Lastly, an obstacle that still needs to be explored in the sensor is the inclusion of Tween in the buffer solution. As stated previously, our buffer solution is composed of 50 mM Tris–HCl, pH 7.4, 100 mM NaCl, 5 mM KCl, 1 mM MgCl2, 0.01% Tween 20 [2]. The Tween in the buffer solution may cause the unraveling of the protein and thus binding patterns which might not occur in the absence of Tween in the solution. Since Tween is a detergent, it is possible that it might have conflicting interactions with the other chemical compounds used not only for the buffer solution but also for the electrode preparation and testing. Our team's planned solution for this potential challenge would be to test the buffer with and without tween in identical trials. If there is a difference in the output values, further investigation will be required into the interactions between detergents and proteins.

To increase data robustness and further validate the feasibility of our concept, it is also important to continue collecting data to achieve a higher sample size. Our team plans to continue testing electrodes with identical procedures in order to validate the use of the sensor across changes in age of aptamer monolayer, change of sample medium, and more. As we push our sensor's capabilities, it will also be of value to introduce an additional transduction method to affirm the calibration of our sensor. As mentioned in previous discussions of reader instrument hardware, our device is equipped with the ability to conduct Impedance Spectroscopy (EIS) as well as the SWV upon which we already rely. EIS can be introduced as a measure to increase sensor accuracy and sensitivity; an EIS calibration curve can be obtained with similar methods as detailed above, and both electrochemical tests can be performed when a sample is introduced. Results can be compared from separate lookup tables to provide a more well-backed result which can be presented to the user with an error calculation, further informing the patient.

Figure 10. Beyond sufficient electrode coverage is achieved by application of a 100uL sample.

Potential Areas for Improvement for Fluidics. When seeking to understand areas of improvement for our design, it is notable that the current design and protocol for user interaction allows them to place their saliva sample on the electrode in a way that is simple, but not necessarily intuitive. These methods have the potential to fail if insufficient saliva is produced or if the user does not fully cover all electrodes. Clearly, it is not a requirement for the user to understand electrochemistry, and it may not necessarily be intuitive to place the saliva covering all three electrodes; thus, it would be a significant improvement if we resolve the requirement for the user to place their own sample on the electrode. Designing another device that is user friendly such that it does not produce a negative user experience, and collects a large saliva sample, would provide an excellent solution. We need to develop a swab that is reusable, and can accurately insert the saliva sample onto the interdigitated electrode. Ideally, this will be integrated with the electrode itself, allowing the user to simply place the chip in their mouth; microfluidics will collect the necessary 55uL and usher it towards the electrodes itself. This will not only create a more positive user experience and remove interaction between the user and the electrode, but it will reduce likelihood of contamination or insufficient sample volume/placement.

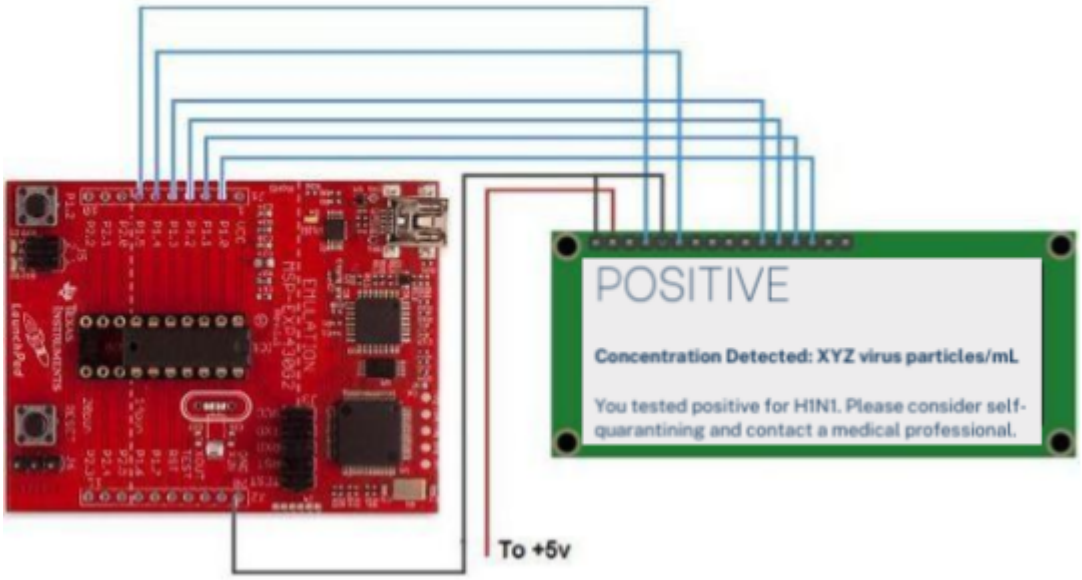

Figure 11. Shows connection between the MSP430 and the output screen for users.

Potential Areas for Improvement of Mobile Electrochemistry Instruments. Designing a separate section of the biosensor that is closed off for temperature measurement would allow for more accurate measurements. This would also allow the electrode to not be affected by the outside temperature and create inaccurate measurements.

Likely, two color sensors would be used- one would be placed at the part of the slot opening where the blue line on the test strip would sit and one deeper in the channel to make sure the test strip color inside the device is correct. This would assist in ensuring the test strip is properly situated in the channel and that only test strips are being inserted into the channel.

Before the electrode is inserted into the device the patient has to handle the electrode which allows for the electrode to be heated (from contact) which will affect temperature measurements. This will create an inaccurate representation of how hot/cold the saliva sample is during testing events. Temperature measurements were performed at the same insertion point of the introduction of the electrode into the sensor pal device. This design allows the electrode to be exposed to the outside environment and also affect temperature measurements.

Finally, the device may be difficult to use for those who are hard of hearing or unable to push a button. In future versions, the directions for use and test results could be announced verbally by the device to direct users. Furthermore, for those who are unable to use press buttons it would be helpful for the device to be able to be directed using voice commands or to be integrated into devices like the Amazon Alexa. This is a point of future development.